Articles

A Versatile Approach to Unimolecular Water-Soluble Carriers: ATRP of PEGMA with Hydrophobic Star-Shaped Polymeric Core Molecules as an Alternative for PEGylation

Oana G. Schramm,[†,‡] Georges M. Pavlov,[†] Hannes P. van Erp,[†] Michael A. R. Meier,[†,‡,⊥] Richard Hoogenboom,[†,‡] and Ulrich S. Schubert*[,†,‡,§]

Laboratory of Macromolecular Chemistry and Nanoscience, Eindhoven University of Technology, P.O. Box 513, 5600 MB Eindhoven, The Netherlands; Dutch Polymer Institute, P.O. Box 902, 5600 AX Eindhoven, The Netherlands; and Laboratory of Organic and Macromolecular Chemistry, Friedrich-Schiller-Universität Jena, Humboldtstr. 10, 07743 Jena, Germany

Received November 4, 2008; Revised Manuscript Received January 15, 2009

ABSTRACT: New amphiphilic star-shaped architectures with dense hydrophilic shells were synthesized by a combination of ring-opening polymerization (ROP) of ε-caprolactone (CL) and atom transfer radical polymerization (ATRP) of different poly(ethylene glycol) methacrylates (PEGMAs). The PCL hydrophobic cores with 4 and 6 arms were near-quantitatively functionalized to 4-, 6-, 8-, and 12-bromine end-capped starPCLs that were subsequently used as macroinitiators for ATRP, leading to the formation of well-defined 4-, 6-, 8-, and 12-arm starPCL*p*PEGMAs. The unimolecular behavior of all 4−12-arm star-shaped block copolymers was unambiguously demonstrated by dynamic light scattering (DLS) and analytical ultracentrifugation (AUC) measurements. Furthermore, no significant aggregation could be detected for the polymers loaded with different hydrophobic molecules as encapsulated guests, proving their carrier abilities in aqueous solutions. Cumulative advantages of the polyPEGMA functionalized systems, such as high hydrophilicity, tunable hydrophobic/hydrophilic balance, and molar masses, make the ATRP of PEGMA a straightforward alternative to the PEGylation approach for drug carrier systems. Furthermore, the dense PEGMA shell suppresses aggregation commonly observed for PEGylated carriers.

Introduction

Based on the original "drug-delivery" concept introduced by H. Ringsdorf in 1981,[1] significant efforts have been directed to increase the efficiency of pharmaceutically active compounds by attempting to control the temporal as well as spatial drug distribution in vivo,[2] evolving into the new interdisciplinary research area of polymer therapeutics.[3] One of the most important general characteristics of such drug-delivery systems is their water solubility since many of the clinically used drugs are hydrophobic or only weakly water-soluble and do, therefore, require a carrier to facilitate their transport through the physiological aqueous media while, at the same time, protecting the sensitive drugs from the harsh conditions in vivo (low pH, oxidative or enzymatic degradation).

Poly(ethylene glycol) (PEG) is the most common solubilizing moiety used to modify a large number of drugs and other therapeutic active compounds in order to enhance their stability and plasma half-life and to reduce their immunogenicity in vivo.[4] On the other hand, the relatively low molar masses achieved by PEGylation of drugs or therapeutic proteins may not allow these systems to circulate long enough through the body in order to reach their target sites due to the high clearance rate characteristic for compounds with molar masses below 20 kDa and limit, at the same time, the passive targeting of such systems (enhanced permeability and retention effect).[5] Furthermore, the hydrophilic/hydrophobic content should be carefully balanced in order to avoid undesired aggregation of the drug carriers. Recent examples of PEGylated polymeric or dendritic cores[6−9] showed that tuning the hydrophilicity of these systems might be rather difficult and that nonspecific supramolecular aggregation cannot always be suppressed. Moreover, similar to the critical micelle concentration (cmc) of the self-assembled micelles of amphiphilic block copolymers, a critical aggregation concentration (cac)[9,10] was observed even for PEGylated dendrimers. The latter case is rather surprising since dendrimers are known to exhibit unimolecular behavior in solution over a wide concentration range. A potential solution to these problems could be the increase of the PEG's molar mass. However, it has been shown that higher molar mass PEGs are more difficult to eliminate from the organism, resulting in undesired polymer accumulation in the body.[11,12] In conclusion, besides the generally accepted benefits of PEGylation, several solubility and stability issues might arise that need to be addressed.

In recent years, well-defined poly[poly(oligoethylene glycol)-methacrylate]s (pPEGMAs) have been prepared by atom transfer radical polymerization (ATRP)[13,14] and reversible addition−fragmentation chain transfer (RAFT).[15,16] The attachment of such well-defined polygrafted short PEG chains to

* Corresponding author. E-mail: u.s.schubert@tue.nl or ulrich.schubert@uni-jena.de.
† Eindhoven University of Technology.
‡ Dutch Polymer Institute.
§ Friedrich-Schiller-Universität Jena.
⊥ Current address: University of Applied Sciences Oldenburg/Ostfriesland/Wilhelmshaven Fachbereich Technik, Constantiaplatz 4, 26723 Emden, Germany.

10.1021/ma8024738 CCC: $40.75
Published on Web 02/23/2009

Scheme 1. Schematic Representation of the Synthetic Approach to Amphiphilic 4- and 6-Arm Star-Shaped Block Copolymers

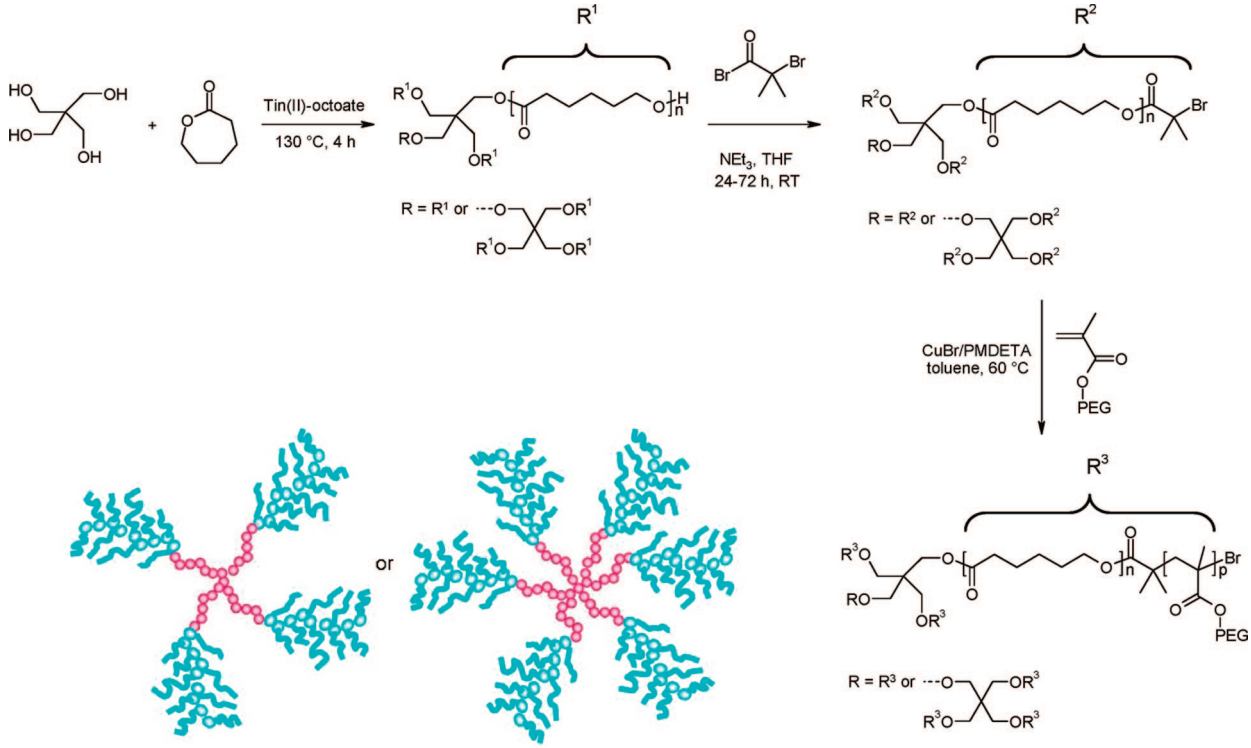

different hydrophobic molecules could synergistically make use of the high hydrophilicity of the multiPEG chains and the ease of increasing the molar masses for prolonged circulating times and passive targeting. Haddleton et al. used a "grafting on" method to attach *N*-succinimidyl end-capped pPEGMA to the amino group of lysozyme as a model protein.[17] The general scope of the pPEGMA attachment can be extended to other hydrophobic cores bearing hydroxy groups, such as dendrimers, polymers, or drugs, by using a "grafting from" method. In particular, for drug-delivery applications, where the drug is not covalently bound to the carrier molecule, star-shaped polymers may have several advantages over other commonly studied drug vehicles such as self-assembled micelles or dendrimers. Compared to self-assembled micelles, both core−shell dendrimers and polymeric unimolecular micelles provide a higher stability in solution since these unimolecular micelles contain covalently fixed branching points.[18,19] On the other hand, the transport abilities of the dendrimers as monodisperse macromolecules may be rather limited, and the tedious, high-cost multistep synthesis could restrict their large-scale applications.

Besides the drug-carrier applications, the transport abilities of the star polymers have been successfully exploited for other areas, such as stimuli responsive release,[20] catalysis,[21,22] imaging,[23] or phase transfer.[24,25] For all these purposes and in particular for biomedical applications, tailor-made polymer structures are required. Controlled polymerization techniques including ring-opening polymerization (ROP)[26,27] and ATRP[28,29] are certainly very powerful and versatile tools to access these linear as well as branched architectures.

Therefore, we investigated a new synthetic strategy combining the ROP of ε-caprolactone using pentaerythritol and dipentaerithritol as initiators for the synthesis of 4-arm and 6-arm hydrophobic core molecules, respectively, with the application of ATRP for the synthesis of the hydrophilic shell using bromine end-capped star-shaped PCL as macroinitiators and different PEG methacrylate monomers (Scheme 1). The hydrophilicity can be even further increased by functionalizing the 4- and 6-arm star-shaped PCL with a branching agent having two ATRP initiating sites, resulting in polymers with twice the number of *p*PEGMA chains per PCL arm, namely 8 and 12 (Scheme 2). The hydrophobic core plays also an important role for the transport abilities of the drug carriers, since the loading capacity depends on the core size and its flexibility. Furthermore, the temporal control over the drug distribution in the organism could be achieved by the use of biodegradable cores. Besides its ability to encapsulate water-insoluble molecules by most likely hydrophobic−hydrophobic interactions, the PCL core offers the great advantage of a well-controlled release of the encapsulated molecules by PCL biodegradation.[30] The total size of the carrier is chosen above 20 kDa to ensure long circulation times while the degradation products are below 20 kDa, allowing clearance from the body.

Experimental Part

Materials. All reagents were used without further purification unless stated otherwise. Solvents were purchased from Biosolve Ltd. (Valkenswaard, The Netherlands). Pentaerythritol, dipentaerithritol, stannous octoate, ε-caprolactone poly(ethylene glycol) methyl ether methacrylate (PEGMA), copper bromide, and *N*,*N*,*N*′,*N*′,*N*″-pentametyldiethylenetriamine (PMDETA) were purchased from Aldrich (Oakville, ON, Canada).

Instrumentation. GPC was measured on a Shimadzu system equipped with a SCL-10A system controller, a LC-10AD pump, a RID-10A refractive index detector, a SIL-10AD autosampler, and a Polymer Laboratories Mixed-D column utilizing a chloroform: triethylamine:isopropanol (93:5:2) mixture as eluent at a flow rate of 1 mL/min and a column temperature at 50 °C. Calibration was performed utilizing linear poly(ethylene glycol) standards.

UV/vis spectra were recorded on a FlashScan S12 (Analytik, Jena, Germany) in 96-well microtiter plates (polypropylene, flat bottom) from Greiner (Greiner Bio-One, Germany) in a range from 250 to 700 nm. All spectra were referenced to an empty microtiter plate, and measurements were performed with four flashes. The actual time for the measurement of one microtiter plate with 96 full UV/vis spectra was ∼40 s.

NMR spectra were measured on a Varian Gemini 400 NMR spectrometer in $CDCl_3$. The chemical shifts were calibrated to TMS.

Scheme 2. Schematic Representation of the Synthetic Approach to Star-Shaped Block Copolymers with 8- and 12-*p*PEGMA Arms Using a Branching Agent

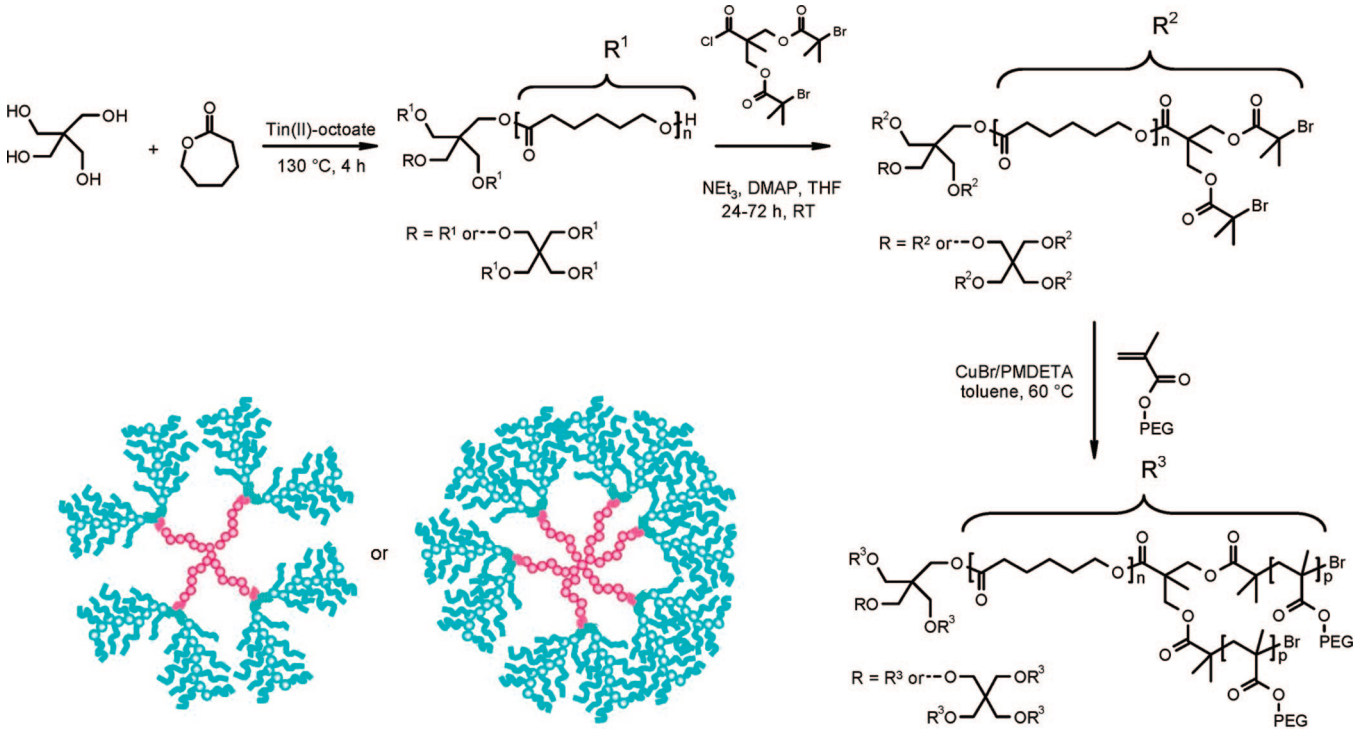

Table 1. Reaction Conditions for the ATRP of PEGMA Using 4−12-Bromine End-Capped StarPCL

macroinitiator	[monomer]/[initiator]	[monomer] [M]	toluene [mL]	[monomer]/[catalyst]/[PMDETA]
4-Br end-capped starPCl	200:1	0.25	20	1:1:1
6-Br end-capped starPCL	240:1	0.25	24	1:1.5:1.5
8-Br end-capped starPCL	400:1	0.25	20	1:2:2
12-Br end-capped starPCL	600:1	0.25	24	1:3:3

DLS measurements were performed on a Brookhaven Instruments Corp. BI-200 apparatus equipped with a BI-2030 digital correlator and a Spectra Physics He−Ne laser with a wavelength of 633 nm. The scattering angle used for the measurements was 90°. The experimental correlation function was analyzed by the method of the cumulants, as described elsewhere.[31] The Stokes−Einstein approximation was used to convert the diffusion coefficient into the hydrodynamic radius (R_h).

Analytical ultracentrifugation was performed on a ProteomeLabTM XL-I (Beckman Coulter) with a rotor speed of 55 000 rpm in a double sector cell with 12 mm optical path length using interference and absorbance optics. Sedimentation coefficients s and frictional ratios (f/f_{sph}) were obtained with the Sedfit program.[32] Thereby, f is the translational friction coefficient of the macromolecules and f_{sph} the translational friction coefficient of a sphere with the same volume.[38] The sedimentation coefficients were determined for each sample at three concentrations. The ranges of concentration provide a reliable extrapolation to zero concentration following the relationship $s^{-1} = s_0^{-1}(1 + k_s c)$, when s_0 is the extrapolated value of the velocity sedimentation coefficient and k_s is the concentration sedimentation coefficient.

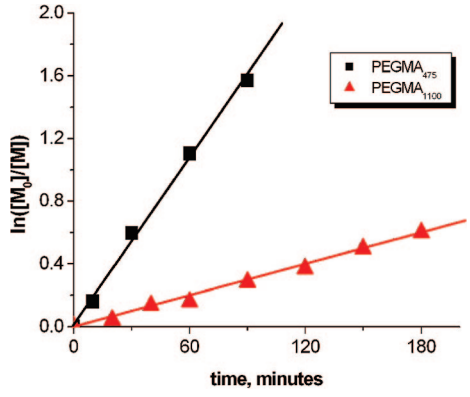

Figure 1. Semilogarithmic kinetic plot for ATRP of different PEGMA monomers using 8-arm macroinitiator, CuBr/PMDETA as catalyst ([I]/[CuBr]/[PMDETA] = 1:2:2), at 60 °C, in toluene.

Viscosity measurements were performed at 25.0 °C using a capillary viscometer. The relative viscosity η_r of the solutions was calculated from the equation $\eta_r = \eta/\eta_0 = t/\tau_0$, where η and t refer to the viscosity and flow time through the capillary of the polymer solution, respectively, and η_0 and τ_0 to the viscosity and the flow time through the capillary of the pure solvent. The ratio η_r was used to determine the specific viscosities: $\eta_{sp} = \eta_r - 1$. The intrinsic viscosity, $[\eta]$, of the copolymer samples was determined both from the Huggins and Kraemer equations.[38,43]

The density increment or buoyancy factor $\Delta\rho/\Delta c$ was measured with a density meter DMA 02 (Anton Paar, Graz, Austria) according to the procedure of Kratky et al. using the equation $\Delta\rho/\Delta c = (1 - \upsilon\rho_0)$, where $\Delta\rho$ is the difference between the densities of the copolymer solution ρ and the pure solvent ρ_0 and υ is the partial specific volume of the copolymer macromolecules.[33]

General Procedure for the Synthesis of 4- and 6-Arm StarPCL-OH. Ring-opening polymerizations of ε-caprolactone were performed at 130 °C for 8 h using 20.00 g (20.60 mL, 0.18 mol) of monomer. The initiator amount was calculated according to the M/I ratio of 48:1 and 72:1, respectively. The monomer, ε-caprolactone, and the initiator, pentaerythritol for 4-arm starPCL-OH or dipentaerythritol for 6-arm starPCL-OH, were added to a flask and stirred for 15 min at 130 °C in order to obtain a homogeneous solution. Subsequently, the polymerization was started by adding the catalyst, stannous octoate (n(cat.) = 1/20 of n(OH-functional groups)). After the reaction time was elapsed the very viscous reaction mixtures were cooled in an ice bath to stop the polymerization. The polymers were purified from residual monomer and catalyst by precipitation from a concentrated dichlo-

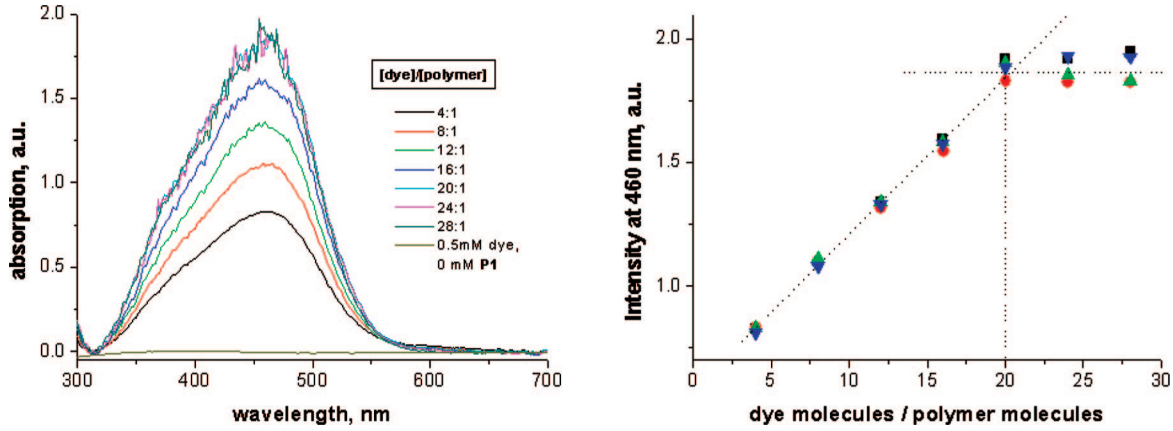

Figure 2. UV/vis spectra obtained from the titration of polymer **P1** with fat brown RR in water (left) and the absorption intensity plotted as a function of the number of encapsulated molecules (right). The titration was performed in quadruplicate.

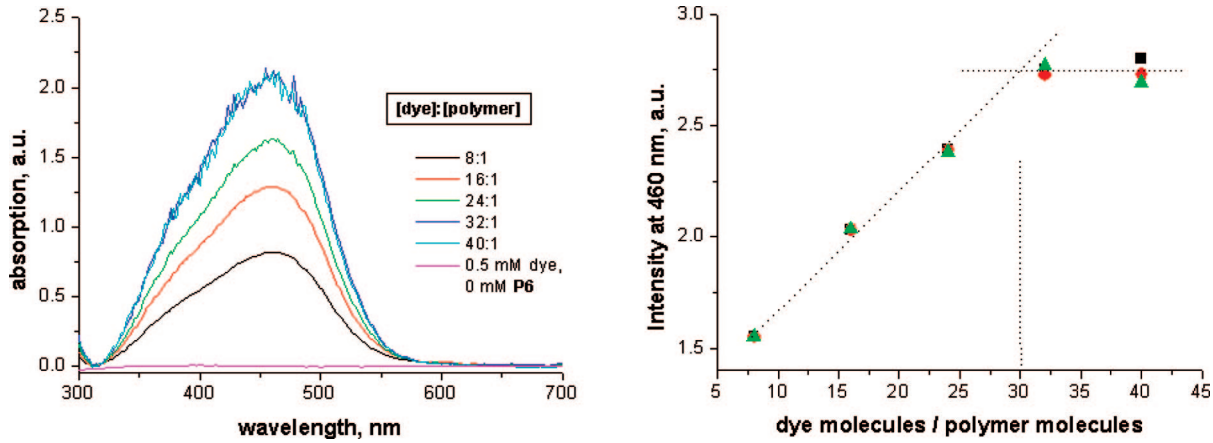

Figure 3. UV/vis spectra obtained from the titration of polymer **P6** with fat brown RR in water (left) and the absorption intensity plotted as a function of the number of encapsulated molecules (right). The titration was performed in triplicate.

romethane solution into ice-cold methanol, resulting in powdery products. The yields were in the order of >95%.

General Procedure for the Synthesis of 4- and 6-Bromine End-Capped Macroinitiators. To a stirred solution of starPCL-OH (1.0 mmol; 5.6 g of 4-arm starPCL-OH or 8.5 g of 6-arm starPCL-OH) and triethylamine (2.0 mmol/arm in 200 mL of dry THF), 2.0 mmol/arm of 2-bromoisobutyryl bromide was added dropwise. The reaction was performed at room temperature for 48−72 h. The reaction mixture was filtrated through a short pad of neutral alumina to remove the quaternary ammonium salts. After the solvent evaporation and precipitation from a small amount of THF in cold methanol, white powdery polymers were obtained in near-quantitative yield.

General Procedure for the Synthesis of 8- and 12-Bromine End-Capped Macroinitiators. To a stirred solution of starPCL-OH (1.0 mmol; 5.6 g of 4-arm starPCL-OH or 8.5 g of 6-arm starPCL-OH), triethylamine and 4-(dimethylamino)pyridine (2.0 mmol/arm in 200 mL of dry THF), 2.0 mmol/arm of the branching agent, 2-(chlorocarbonyl)-2-methylpropane-1,3-diyl bis(2-bromo-2-methylpropanoate),[35] was added dropwise. The reaction was performed at room temperature for 48−72 h. The reaction mixture was filtrated through a short pad of neutral alumina to remove the quaternary ammonium salts. After the solvent evaporation and precipitation from a small amount of THF in cold methanol, white powdery polymers were obtained in near-quantitative yield.

General Procedure for the Synthesis of 4−12-Arm StarPCL-*p*PEGMAs. The catalyst CuBr and the ligand PMDETA were added to 5 mL of toluene previously purged with argon for 10 min. A solution of macroinitiator and PEGMA monomer in 15 or 19 mL of toluene (Table 1) was purged with argon for 10 min and then added to the catalyst suspension. The amount of the initiator was calculated according to the M/I ratios (monomer concentration 0.25 M, Table 1). The reaction mixture was then stirred for 3−5 h at 60 °C under an inert atmosphere. The reaction was stopped by cooling to room temperature and dilution with toluene in air. The content was then passed through a short pad of alumina to remove the copper catalyst. After solvent evaporation, the polymer was precipitated from a small amount of toluene in diethyl ether, filtered, and dried under vacuum for several hours. The degree of polymerization (DP) of PEGMA related to the DP of PCL (12/arm) was determined by ^{1}H NMR spectroscopy from the integrated ratios of the signal at 4.1 ppm corresponding to the resonances of the methylenic protons from the PCL core and the signals at 3.4 ppm assigned to the methoxy protons from the starPCL-*p*PEGMAs. The molar masses of all star-shaped polymers were calculated according to the DP of the PCL, DP of the *p*PEGMA shell, and the number of arms.

General Procedure for Determination of the ATRP Kinetics Using 4−12-Bromine End-Capped StarPCL Macroinitiators by ^{1}H NMR Spectroscopy. The ATRP of PEGMA using 4−12-bromine end-capped starPCL macroinitiators was performed according to the general procedure described previously. Aliquots of 0.2−0.3 mL were taken from the reaction mixture every 10−20 min. The content was then passed through a short pad of alumina and washed with 2−3 mL of toluene, in air, in order to remove the copper catalyst and to stop the polymerization. After solvent evaporation, 6 mL of $CDCl_3$ was added to the reaction mixture, and ^{1}H NMR spectra were recorded for each aliquot. The resonance at 3.1 ppm corresponding to the methoxy protons from the formed polymer and the methoxy protons from the monomer was calibrated to 100. The monomer conversions were then calculated subtracting from 100 the percentages of unreacted monomer (determined from

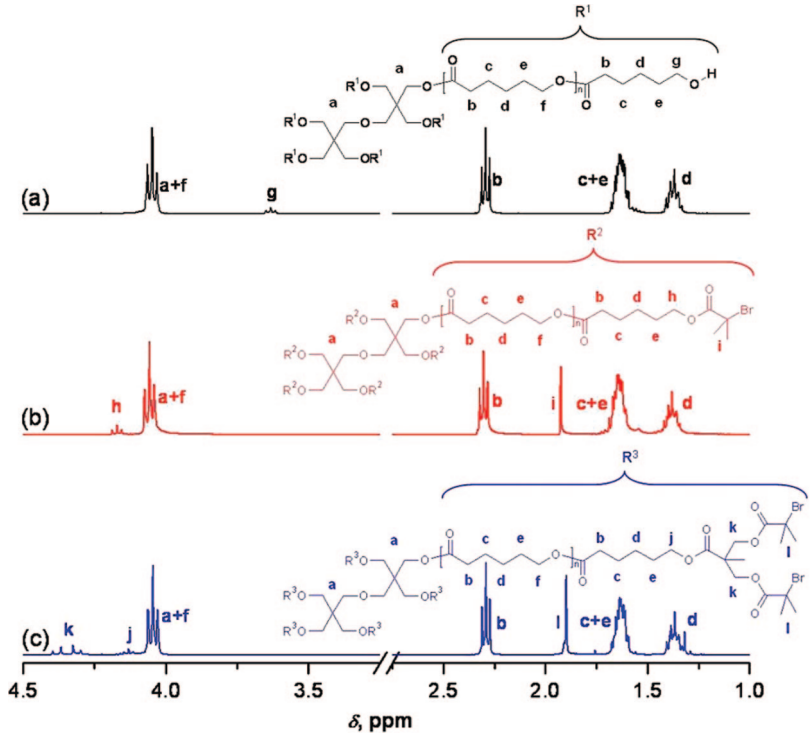

Figure 4. Representative ^{1}H NMR spectra of 6-arm starPCL-OH, (a) 6-arm starPCL-1-Br (b), and 6-arm starPCL-2-Br (c) in $CDCl_3$.

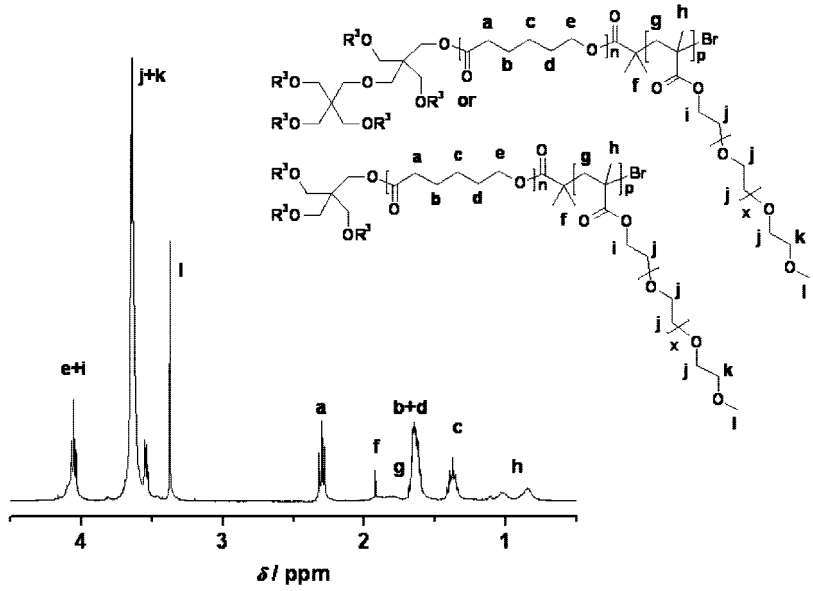

Figure 5. Representative ^{1}H NMR spectrum for 4- and 6-arm star-PCL-*p*PEGMA in $CDCl_3$.

Table 2. General Characterization of Multiarm StarPCL-*p*PEGMAs

polymer	no. of arms (PCL core)	no. of arms (PEGMA shell)	DP of PEGMA per arm	M_w PEGMA [g/mol]	M_n (GPC) [g/mol]	M_n (^{1}H NMR) [g/mol]	PDI (GPC)	conv [%]
P1	4	4	30	475	30 700	63 200	1.16	60
P2	4	8	21	475	41 000	87 000	1.11	42
P3	6	6	18	1100	37 000	128 000	1.10	42
P4	6	12	8	475	28 000	56 000	1.08	16
P5	6	12	9	475	29 000	69 000	1.08	18
P6	6	12	13	475	32 500	85 000	1.08	26
P7	6	12	13	1100	45 000	182 500	1.12	28

the integrated olefinic signals at 6.2 and 5.6 ppm). Subsequently, the conversions were semilogarithmically plotted versus time (minutes, Figure 1).

General Procedure for the UV/vis Polymer Titrations. For the preparation of a [4]:[1] molar ratio [dye]/[polymer] aqueous solution, 5.25 mg (0.02 mmol) of fat brown RR was added to a solution of polymer, 0.005 mmol, in 100 mL of demineralized water. After ultrasonication for 2 min at 40 °C when the dye was completely dissolved, 10 mL of this solution was placed into a separated vial. To the rest of the solution 4.72 mg of dye was added, corresponding to a [dye]/[polymer] ratio of [8]:[1], and after ultrasonication at 40 °C for 2 min, another 10 mL was placed into

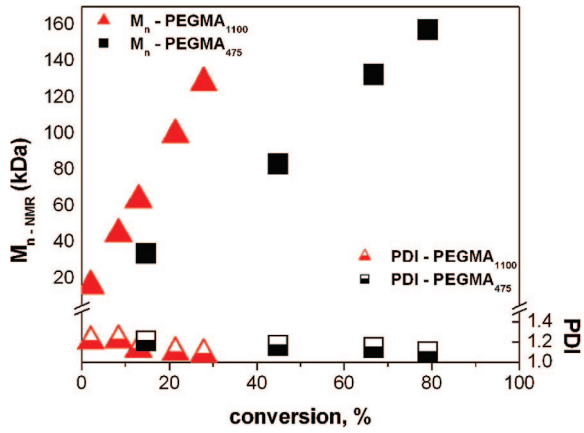

Figure 6. M_n (determined from ^{1}H NMR) and PDI (determined from GPC) during ATRP of different PEGMA monomers, using the 8-arm macroinitiator, CuBr/PMDETA as catalyst ([I]/[CuBr]/[PMDETA] = 1:2:2), at 60 °C, in toluene.

a separated vial. The procedure has been repeated for all seven solutions of different [dye]/[polymer] ratios. The solutions were then diluted with 30 mL of water, and their UV/vis absorptions were measured. A control UV/vis spectrum was recorded for a suspension of 1.21 mg of dye in 10 mL of water (0.5 mM) in the absence of polymer (see Figures 2 and 3).

Results and Discussion

Hydrophobic PCL cores with 4 and 6 arms having 12 repeating units of caprolactone per arm were synthesized by ROP using pentaerithritol and dipentaerithritol as initiators (Scheme 1).[34] After purification, the starPCL-OHs were fully converted to bromine end-capped starPCLs by the reaction with 2-bromoisobutyryl bromide or with the branching agent, 2-(chlorocarbonyl)-2-methylpropane-1,3-diyl bis(2-bromo-2-methylpropanoate),[35] in THF at room temperature. Figure 4 depicts the representative ^{1}H NMR spectra of the starPCL-OH and the starPCL-Br macroinitiators. The complete shift of the signal assigned to the methylenic protons adjacent to the hydroxyl group in the ^{1}H NMR spectrum of the starPCL-OH from 3.65 ppm to lower field (4.19 ppm) in the ^{1}H NMR spectra of the both starPCL-Brs as well as the appearance of the new methyl and methylenic signals at 1.9 and 4.30 ppm indicates the near-quantitative conversion of the starPCL-OH to bromine end-capped starPCLs.

A series of amphiphilic multiarm star-shaped poly(caprolactone)-*b*-poly(ethylene glycol methyl acrylate)s (starPCL-*p*PEGMA) with two different molar masses of PEGMA (M_w 475 and M_w 1100) and various sizes of the hydrophilic shell were synthesized using bromine end-capped starPCLs as macroinitiators (Table 2). In all cases well-defined polymers with narrow polydispersity indices (PDI 1.08−1.16) were obtained by choosing proper M/I ratios, a low monomer concentration (0.25 M), a moderate temperature (60 °C), and low catalyst contents (molar ratios of 4-, 6-, 8-, and 12-arm macroinitiator/CuBr/PMDETA 1:1:1; 1:1.5:1.5; 1:2:2, and 1:3:3, respectively).

Figure 5 displays a typical ^{1}H NMR spectrum for the star-PCL-*p*PEGMAs. The signals at ∼3.4 ppm can be easily assigned to the protons of the methoxy end group of the PEGMA, while the signals at ∼1.36, 1.64, 2.3, and 4.02 ppm are characteristic for the methylenic protons from the PCL. From the integral ratios of these signals the composition as well as the M_n of the multiarm star polymers could be determined.

In addition, ^{1}H NMR analysis of the monomer conversion as a function of time and the molar mass versus conversion revealed first-order kinetics, as expected for a controlled radical polymerization process[28,29] (Figures 1 and 6).

The gel permeation chromatography (GPC) traces of all synthesized polymers showed monomodal and symmetric molar mass distributions, indicating that star−star coupling reactions could be minimized under the optimized conditions. However, the lowest polydispersity indices (1.08−1.10) were obtained for lower monomer conversions (Figure 7).

GPC and ^{1}H NMR spectroscopy were used for the structural characterization of all polymers (Figures 2 and 5). However, with these methods it was not possible to accurately determine whether all of the bromine end-capped arms initiated the ATRP of PEGMAs. Therefore, the ATRP was monitored in time by ^{1}H NMR spectroscopy, revealing that all bromine end-capped groups initiated the ATRP since more than 90% of the methylenic signals at ∼4.19 ppm in the ^{1}H NMR spectrum of the macroinitiator were shifted in about 30 min to higher fields upon the *p*PEGMA chain growth, and after 60 min no significant signal could be detected anymore at 4.19 ppm (Figure 8).

The carrier and solubilization abilities of all star-shaped polymers were investigated using the water-insoluble dye fat brown RR (4-(naphthalene-1-yldiazenyl)benzene-1,3-diamine) as model compound, by the evaluation of changes in its microenvironment utilizing UV/vis spectroscopy. Different aqueous solutions of constant polymer concentration and increasing dye concentrations have been prepared for the UV/vis titration experiments (Figures 2, 3 and 9). A control UV/vis measurement of the dye in water clearly showed that no absorption maximum can be detected in the absence of polymer since the dye is water-insoluble (Figures 2 and 3).

Upon titration of the aqueous stock solution of 25 μM of polymer with fat brown RR, the absorption intensity at 460 nm

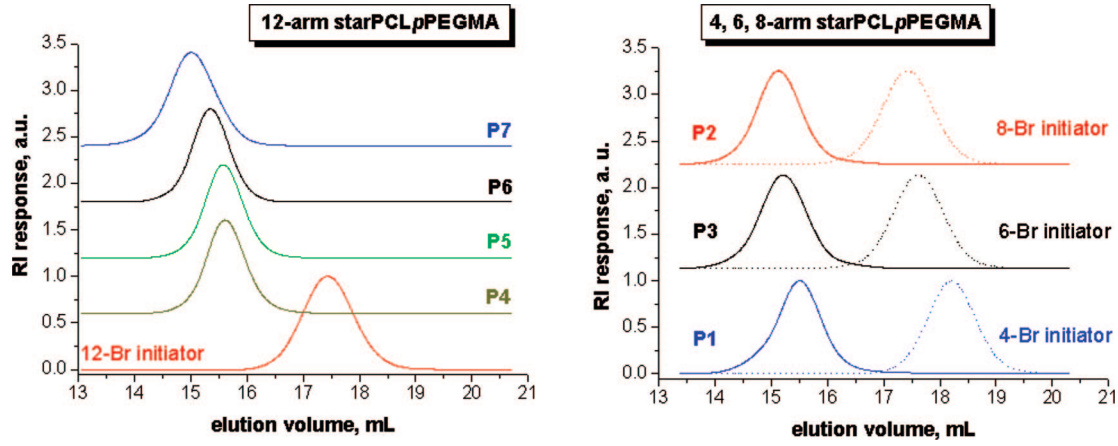

Figure 7. GPC traces of starPCL-*p*PEGMA, **P1**−**P7**.

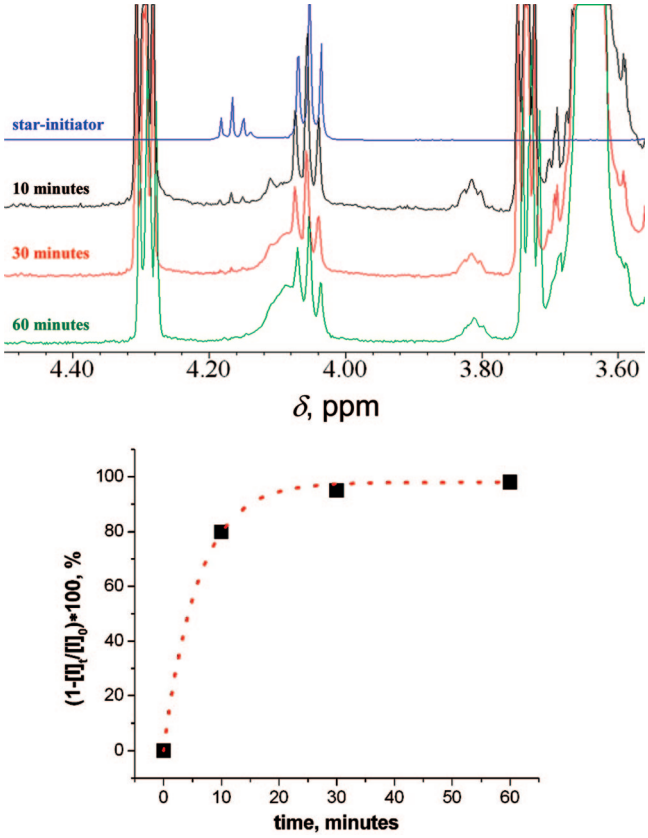

Figure 8. ^{1}H NMR spectra of the reaction mixture during the polymerization in $CDCl_3$ (top). Disappearance of the initiating groups in time (bottom).

(λ_{max}) significantly increased, indicating the encapsulation and the solubilization of the dye by the polymer (Figures 8 and 9). The intensity at 460 nm increased almost linearly with the concentration of fat brown RR until the polymer molecules were overloaded with guest molecules and scattering effects due to undissolved dye molecules were observed. Thus, the maximum loading capacity of about 20 dye molecules per molecule of polymer was found for the star-shaped polymers with a 4-armPCL core and 30 dye molecules per molecule of polymer with a 6-arm PCL core (Figure 9).

The higher loading capacity of the polymers with a 6-arm PCL corona can be interpreted as a consequence of their larger hydrophobic compartment that is able to encapsulate by hydrophobic−hydrophobic interactions more guest molecules than the corresponding polymers with a 4-arm PCL corona. It has been found that the size and the density of the hydrophilic shell do not influence the maximum loading capacities of the polymers; the hydrophilic shell just prevents the supramolecular aggregation before and upon loading the polymer with guest molecules.

Dynamic light scattering (DLS) measurements confirmed the unimolecular micelle behavior for all 4−12-arm star-shaped block copolymers with and without guest molecules. The slight increase of the hydrodynamic diameter up to 25% upon loading the polymers with dye molecules (Table 3) and the absence of larger supramolecular aggregates indicate that the guest molecules are incorporated inside the polymer molecule.

Furthermore, analytical ultracentrifugation (AUC) measurements support the dye encapsulation inside the polymer molecule. Similar differential distribution of sedimentation coefficients (corresponding to similar molar masses, as the friction ratios are almost constant) for loaded and unloaded polymers were determined by velocity sedimentation analysis

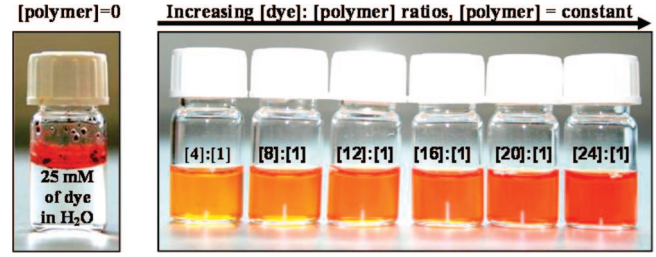

Figure 9. Different aqueous solutions for the titration of polymer **P1** with fat brown RR.

Table 3. General Characterization of Multiarm StarPCL-*p*PEGMAs

polymer	P1	P2	P3	P4	P5	P6	P7
R_h-DLS (polymer without dye) [nm]	5.4	5.8	6.4	6.3	6.4	6.5	6.9
R_h-DLS (polymer with dye) [nm]	6.8	6.0	6.8	7.5	7.2	6.6	6.9

Table 4. Velocity Sedimentation Coefficient (s_0), Concentration Coefficient (k_s), Frictional Ratio (f/f_{sph}), Intrinsic Viscosity, and Molar Mass (M_{sf}[a]) of Multiarm StarPCL-*p*PEGMAs Determined by AUC and Viscometry (THF as Solvent)

polymer	$s_0 \times 10^{13}$ [s]	k_s [cm^3/g]	f/f_0	η [cm^3/g]	$M_{sf} \times 10^{-3}$ [g/mol]
P1	6.3	35	1.26	15.5	44
P2	8.2	21	1.30	15.6	68
P3	8.8	46	1.40	15.0	84
P4	5.5	43	1.50	15.2	46
P5	5.9	35	1.40	15.2	46
P6	7.2	37	1.65	15.1	80
P7	10.9	48	1.30	16.0	104

[a] Molar masses from the velocity sedimentation analysis were determined by modified Svedberg relations: $M_{sf} = 9\pi 2^{1/2} N_A([s](f/f_{sph})_0)^{3/2} v^{1/2}$, where N_A is the Avogadro number and v is the partial specific volume of the polymer.

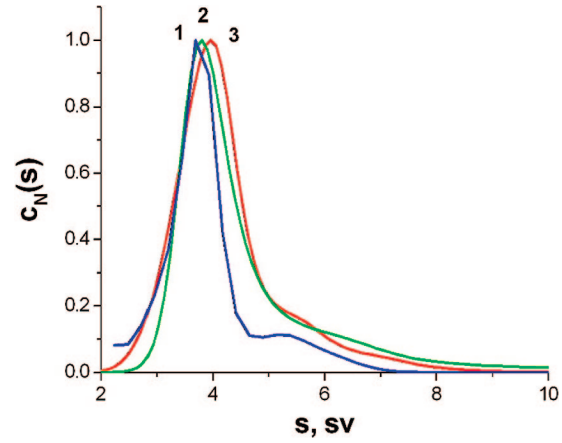

Figure 10. Normalized differential distribution of sedimentation coefficients of polymer **P7** loaded or unloaded with guest molecules: (1) interference, polymer without dye; (2) absorbance (λ = 460 nm), polymer with dye; (3) interference, polymer with dye.

using two different methods of boundary registrations: interference and absorbance (Figure 10).

The small shoulder corresponding to higher molar masses in the AUC analysis of the polymer without guest molecule suggests that the star−star coupling could not be completely suppressed during the ATRP, although no similar peak could be detected by GPC.

Molar masses from the velocity sedimentation analysis were determined by modified Svedberg relations: $M_{sf} = 9\pi 2^{1/2} N_A([s](f/f_{sph})_0)^{3/2} v^{1/2}$, where N_A is Avogadro number and v is the partial specific volume of polymer (Table 4).

Besides the molar mass determination, the AUC provides also useful information about the behavior of the polymers in

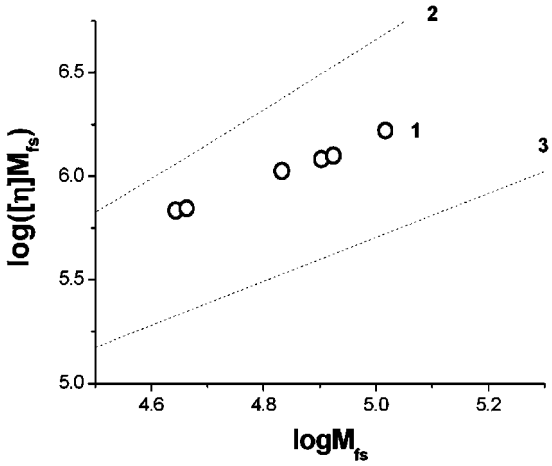

Figure 11. Dependence of the hydrodynamic volume $[\eta]M$ vs M on double-logarithmic scale for different polymer systems: (1) multiarm starPCL-*p*PEGMAs molecules and (2) flexible linear polymers in thermodynamically good solvents as well as (3) dendrimers, glycogen, and globular proteins.

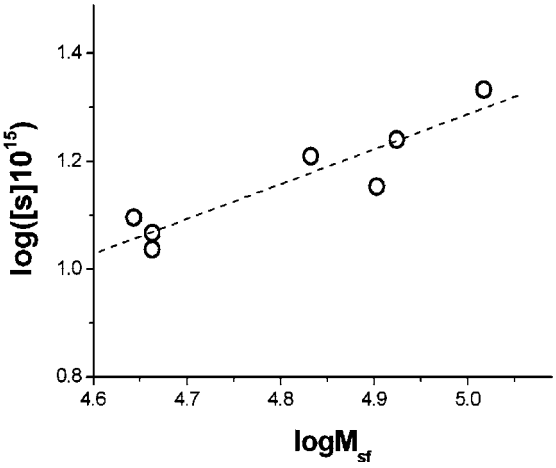

Figure 12. Double-logarithmic plot of the intrinsic velocity sedimentation coefficient $[s] \equiv s_0\eta_0/(1 - \upsilon_0)$ vs molar mass M_{sf} of the multiarm starPCL-*p*PEGMAs molecules in THF. Dashed line may be described by the following relationship: $[s] = 1.109 \times 10^{-17}M^{0.65\pm0.10}$.

different solvents (the hydrodynamic volume, the possible shape, etc.). Thus, the product $[\eta]M$ represents the hydrodynamic volume occupied by macromolecules in solutions. The hydrodynamic volume versus molar mass plots for the multiarm starPCL-*p*PEGMAs molecules are situated between the values determined for linear macromolecules[36,37] and globular proteins[38,39] or dendrimers[40,41] (Figure 11), indicating that the multiarm starPCL-*p*PEGMAs molecules are more compact in comparison with the linear macromolecules of the same molar mass and less compact in comparison with dendrimer molecules. At the same time, for the multiarm starPCL-*p*PEGMAs molecules we observed that $[\eta]M \sim M^{1.0}$, and the volume occupied by the macromolecules is proportional to its molar mass. This behavior is characteristic for globular proteins and dendrimers.[42] However, the multiarm starPCL-*p*PEGMAs molecules occupy larger volumes than dendrimer molecules. This finding suggests that star-shaped polymers can encapsulate more guest molecules than dendrimers. The double-logarithmic plots of the hydrodynamic data (velocity sedimentation coefficient and intrinsic viscosity) versus molar mass (Figures 11 and 12) reveal that this set of parameters might be considered at the first approximation, as the homologous series $s \sim M^{b_s} \sim M^{0.65\pm0.10}$ (with the linear correlation coefficient $r = 0.924$) and $[\eta] \sim M^{b_\eta} \sim M^{\cong 0}$ ($r = 0.998$). The ratio between the scaling indexes follows the general rule for the homologous series:[43] $b_s = (2 - b_\eta)/3$.

Conclusions

New unimolecular core−shell architectures with increased hydrophilicity were successfully synthesized by a "grafting from" method. Their unimolecular character and the transport abilities were unambiguously demonstrated by UV/vis spectroscopy, DLS, and AUC analyses, proving their potential as nanocarriers. The core biodegradability and the biocompatibility of the shell building blocks make the multiarm star-shaped PCL*p*PEGMAs suitable for biological applications. The increased hydrophilicity and molar masses gained by *p*PEGMA attachment designate this approach as a straightforward alternative to PEGylation methods. The resulting PEGylated nanocarriers exhibited high loading capacities that depend on the core size while it is not influenced by the hydrophilic corona, indicating that the encapsulation occurs in the core of the carriers. AUC investigations revealed that the flexibility of these star-shaped polymers is in between the flexibility of linear polymers and dendrimers.

Acknowledgment. The authors thank the Dutch Polymer Institute (DPI) and The Netherlands Organization for Scientific Research (NWO) for financial support.

References and Notes

(1) Gros, L.; Ringsdorf, H.; Schupp, H. *Angew. Chem.* **1981**, *93*, 311−333; *Angew. Chem., Int. Ed.* **1981**, *20*, 347−360.
(2) Qiu, L. Y.; Bae, Y. H. *Pharm. Res.* **2006**, *23*, 1–30.
(3) Duncan, R. *Nat. Rev. Drug Discovery* **2003**, *2*, 347–360.
(4) Ryan, S. M.; Mantovani, G.; Wang, X.; Haddleton, D. M.; Brayden, D. J. *Expert Opin. Drug Delivery* **2008**, *5*, 371–383.
(5) Matsumura, Y.; Maeda, H. *Cancer Res.* **1986**, *46*, 6387–6392.
(6) van de Coevering, R.; Bruijnincx, P. C. A.; van Walree, C. A.; Kleinn; Gebbink, R. J. M.; van Koten, G. *Eur. J. Org. Chem.* **2007**, *293*, 1–2939.
(7) Morara, A. D.; McCarley, R. L. *Org. Lett.* **2006**, *8*, 1999–2002.
(8) Xu, J.; Zubarev, E. R. *Angew. Chem.* **2004**, *1165*607−5612; *Angew. Chem., Int. Ed.* **2004**, *43*, 5491−5496.
(9) Radowski, M. R.; Shukla, A.; von Berlepsch, H. H.; Böttcher, C.; Pikaert, G.; Rehage, H.; Haag, R. *Angew. Chem.* **2007**, *119*, 1287−1292; *Angew. Chem., Int. Ed.* **2007**, *46*, 1265−1269.
(10) Xu, S.; Luo, Y.; Haag, R. *Macromol. Rapid Commun.* **2008**, *29*, 171–174.
(11) Bendele, A.; Seely, J.; Richey, C.; Sennello, G.; Shopp, G. *Toxicol. Sci.* **1998**, *42*, 152–157.
(12) Yurkovetskiy, A.; Choi, S.; Hiller, A.; Yin, M.; McCusker, C.; Syed, S.; Fischman, A. J.; Papisov, M. I. *Biomacromolecules* **2005**, *6*, 2648–2658.
(13) Lutz, J.-F.; Hoth, A. *Macromolecules* **2006**, *39*, 893–896.
(14) Lutz, J.-F.; Akdemir, Ö.; Hoth, A. *J. Am. Chem. Soc.* **2006**, *128*, 13046–13047.
(15) Fournier, D.; Hoogenboom, R.; Thijs, H. M. L.; Paulus, R. M.; Schubert, U. S. *Macromolecules* **2007**, *40*, 915–920.
(16) Becer, C. R.; Hahn, S.; Fijten, M. W. M.; Thijs, H. M. L.; Hoogenboom, R.; Schubert, U. S. *J. Polym. Sci., Part A: Polym. Chem.* **2008**, *46*, 7138–7147.
(17) Lecolley, F.; Tao, L.; Mantovani, G.; Durkin, I.; Lautru, S.; Haddleton, D. M. *Chem. Commun.* **2004**, 2026–2027.
(18) Seymour, L. W.; Miyamoto, Y.; Maeda, H.; Brereton, M.; Strohalm, J.; Ulbrich, K.; Duncan, R. *Eur. J. Cancer* **1995**, *31*, 766–770.
(19) Meier, M. A. R.; Gohy, J.-F.; Fustin, C.-A.; Schubert, U. S. *J. Am. Chem. Soc.* **2004**, *126*, 11517–11521.
(20) Krämer, M.; Stambé, J.-F.; Türk, H.; Krause, S.; Komp, A.; Delineau, L.; Prokhorova, S.; Kautz, H.; Haag, R. *Angew. Chem., Int. Ed.* **2002**, *41*, 4252−4256; *Angew. Chem.* **2002**, *114*, 4426−4431.
(21) Piotti, M. E., Jr.; Bond, R.; Hawker, C. J.; Fréchet, J. M. F. *J. Am. Chem. Soc.* **1999**, *121*, 9471–9472.
(22) Astruc, D.; Chardac, F. *Chem. Rev.* **2001**, *101*, 2991–3023.
(23) Fukukawa, K.; Rossin, R.; Hagooly, A.; Pressly, E. D.; Hunt, J. N.; Messmore, B. W.; Wooley, K. L.; Welch, M. J.; Hawker, C. J. *Biomacromolecules* **2008**, *9*, 1329–1339.
(24) Goetheer, E. L. V.; Baars, M. W. P. L.; van den Broeke, L. J. P.; Meijer, E. W.; Keurentjes, J. T. F. *Ind. Eng. Chem. Res.* **2000**, *39*, 4634–4640.

(25) Cooper, A. I.; Londono, J. D.; Wignall, G.; McClain, J. B.; Samulski, E. T.; Lin, J. S.; Dobrynin, A.; Rubinstein, M.; Burke, A. L. C.; Frechet, J. M. J.; DeSimone, J. M. *Nature (London)* **1997**, *389*, 368–371.
(26) Biela, T.; Kowalski, A.; Libiszowski, J.; Duda, A.; Pêczek, S. *Macromol. Symp.* **2006**, *240*, 47–55.
(27) Mecerreyes, D.; Jérôme, R.; Dubois, P. *Adv. Polym. Sci.* **1999**, *147*, 1–59.
(28) Matyjaszewski, K.; Xia, J. *Chem. Rev.* **2001**, *101*, 2921–2990.
(29) Kamigaito, M.; Ando, T.; Sawamoto, M. *Chem. Rev.* **2001**, *101*, 3689–3745.
(30) Schramm, O. G.; Meier, M. A. R.; Hoogenboom, R.; van Erp, H. H. P.; Gohy, J.-F.; Schubert, U. S. *Soft Matter* **2009**, *5*, in press (DOI: 10.1039/b816087b).
(31) Berne, B. J.; Pecora, R. J. *Dynamic Light Scattering*; John Wiley and Sons: Toronto, 1976.
(32) Schuck, P. *Biophys. J.* **2000**, *78*, 1606–1619.
(33) Kratky, O.; Leopold, H.; Stabinger, H. *Methods Enzymol.* **1973**, *27*, 98–110.
(34) Meier, M. A. R.; Schubert, U. S. *e-Polym.* **2005**, *085*, 1–8.
(35) Breland, L. K.; Storey, R. F. *Polymer* **2008**, *49*, 1154–1163.
(36) Aminabhavi, T. M.; Munk, P. *Macromolecules* **1979**, *12*, 1194–1196.
(37) Horita, K.; Abe, F.; Einaga, Y.; Yamakawa, H. *Macromolecules* **1993**, *26*, 5067–5072.
(38) Tanford, C. *Physical Chemistry of Macromolecules*; Wiley: New York, 1961.
(39) Creeth, J. M.; Knight, C. G. *Biochim. Biophys. Acta* **1965**, *102*, 549–558.
(40) Pavlov, G. M.; Errington, N.; Harding, S. E.; Korneeva, E. V.; Roy, R. *Polymer* **2001**, *42*, 3671–3678.
(41) Pavlov, G. M.; Korneeva, E. V.; Meijer, E. W. *Colloid Polym. Sci.* **2002**, *280*, 416–423.
(42) Pavlov, G. M. *Eur. Phys. J. E* **2007**, *22*, 171–180.
(43) Tsvetkov, V. N.; Eskin, V. E.; Frenkel, S. Y. *Structure of Macromolecules in Solutions*; Butterworths: London, 1970.

MA8024738